

Temperature measurements within the luminous region of a burning $\text{Ba}(\text{NO}_3)_2/\text{Al}$ mixture

P. J. Disimile, R. Prasad and N. Toy

UC-FEST, Department of Aerospace Engineering, University of Cincinnati, Ohio 45221, USA

Abstract: *Knowledge of the local temperature field associated with a pyrotechnic event has numerous implications, especially in the field of safety and survivability. These implications involve the development of sensors that are capable of detecting pyrotechnic events and that are used in part to eliminate or reduce a fire hazard. However, in order to be able to predict a possible fire scenario from a pyrotechnic event the temperature distributions and the thermal heat transfer are prerequisites. This experimental study discusses the temperature measurement methodology required to evaluate the transient temperatures associated with a small, commercially available, pyrotechnic device. Furthermore, the temperature distribution close to the surface of two devices, one commercial, the other fabricated, has been obtained, and shows that the temperature distribution away from the event is not uniform.*

Keywords: *Temperature distribution, thermocouples, pyrotechnic facility*

Introduction

The use of pyrotechnic compositions can be found in numerous fields like rocket propellants, highway flares, entertainment and other high-energy applications. Due to the release of a large amount of thermal energy, the burning composition and the events occurring around a pyrotechnic device are saturated by the intensity of emitted light. Hence a uniform region of light is observed which gives the impression of a fireball of constant temperature throughout. This is even more prominent when considering transient pyrotechnic events such as in the use of fireworks and incendiary devices. The measurement of the high temperatures that are produced by such near instantaneous chemical reaction is difficult to achieve and challenging to understand, and the ability to measure the temperature of a dynamic and transitory thermal field is far from trivial.

In order to be able to measure the expected high temperatures within the flash/fireball of a short duration pyrotechnic event a number of different techniques were considered. Of these, the most notable that have been used are optical pyrometers whereby the brightness of a flame has been compared to the brightness of an incandescent filament in order to determine the flame temperature.¹ Other types of pyrometers have also been used, but have not been successful, for example, cinephoto pyrometer, photoelectric photometer and a

color photometer.¹ In comparison, temperature measurements of complex combustion within non-uniform temperature zones have been used successfully using a line-reversal methodology. However, this method only provides intermediate temperature distributions within the various zones of a flame and is dependent upon the emission of characteristic spectral lines from the flame as viewed by a spectroscope.² However, even in this latter method, the temperature measurements only accounted for the average temperature across a flame region and the variations within the inner zones were unaccounted for. Although temperature fields with relation to flame height have been measured using a cinephoto pyrometer,¹ detailed temperature distributions were unattainable since this method could not provide measurements at intervals less than 10 mm.

In order to satisfy the goals of the present study, it was considered necessary to adopt an approach of using high-speed thermocouples to capture the temperature distribution. Such temperature measurements have been performed earlier at a single fixed position in a closed system on different pyrotechnic materials, notably Sb/ KMnO_4 (antimony/potassium permanganate),³ and Pd/Al (palladium/aluminum) mixtures.⁴ Temperature profiles have also been measured using W/Re (tungsten/rhenium) thermocouples for temperatures above 2000 °C in Mo/ KClO_4 (molybdenum/potassium perchlorate) material,⁵

and W/KClO₄/BaCrO₄ (tungsten/potassium perchlorate/barium chromate) material,⁶ but again only at a fixed position in the system. Although bare bead W/Re type thermocouples are capable of measuring temperatures in excess of 2000 °C, they are very prone to oxidation that can lead to large errors and have to be used within inert environments to prevent the tungsten from oxidizing.

The ability to measure and to analyze the dynamic thermal events surrounding a short duration pyrotechnic is problematical but it was not considered impractical if the temperature range of the apparatus could be obtained and if the thermal response was fast enough to record the event. Given these complications, it was decided to examine the capability of miniature high-speed thermocouples to observe the temperature distribution close to the surface of a pyrotechnic event. Two types of thermocouple were initially chosen for this study, an R- and a K-type which have the ability to measure maximum temperatures up to 1750 °C and 1250 °C respectively. A pyrotechnic event was created using, in the first instance, a common sparkler, and secondly a laboratory made device containing a chemical mixture similar to that of a commercial pyrotechnic material (CPM).

Experimental Strategy

Since thermocouples are available in different combinations of metals or calibrations it was necessary to select ones that were favorable to this study. The four most common types are J, K, T and E, with each type having a different temperature

range and environmental usage, although the maximum temperature that each may record depends on the diameter of the wire used in the thermocouple. Given the harsh environment of the present studies, the following criteria were used in selecting a suitable thermocouple:

- (1) Temperature range: The operating range of a thermocouple is the temperature range over which the thermocouple will perform satisfactorily, with negligible error in the output signal. For the current set of experiments, a temperature range with a high upper measuring limit was desirable.
- (2) Thermocouple junction selection: Each thermocouple must utilize a measuring junction and a reference junction at two different temperatures. The measuring junction is generally at the higher of the two temperatures and the reference junction is at ambient. The measuring junction is placed near or on whatever is to be measured and the reference junction is connected either to a controller or a temperature indicator. Different kinds of measuring junctions are used with respect to measuring requirements as shown in Table 1. From this table it may be observed that for the present study an exposed bead weld, with a low thermal mass and corresponding fast response time, would be the most acceptable geometry for a thermocouple.
- (3) Response time using first order response criteria: The time constant is the time required for the measured temperature to reach 63.2%

Table 1 Effect of different thermocouple constructions.

Type of junction	Response time	Advantages	Disadvantages	
Sheathed	Ungrounded	Slow	Reliable and rugged construction	Sluggish response time
	Grounded	Normal	Useful for electrically conductive metallic sheaths	Noise injection
Exposed	Bead weld	Fast	Low thermal mass increases response time	Prone to damage in a corrosive environment
	Butt weld	Fastest	Useful in high speed measurements	Corrosive failure and physical or mechanical damage

of a step change in the temperature of the surrounding media. Five time constants are required for the sensor to approach 100% of the step change value. Typical response time for thermocouples range from milliseconds to seconds, depending on the size of the thermocouple, the fluid thermal conditions and the junction employed.

- (4) Operating environment: The operating temperature and external environment can affect the performance of the thermocouple. The present test conditions required thermocouples whose output signals were not affected by any particulate from the flash/fireball scenario.

In order to record the temperature measurement from the selected thermocouple a dedicated acquisition system was used. This consisted of a 16-channel analog to digital data acquisition system with 12-bit resolution (National Instruments PXI - E6040E) that was connected to a stand-alone personal computer. LabVIEW software controlled the data acquisition program in such a way that different types of thermocouples could be accommodated using a single input channel. This approach was adopted so that the two types of thermocouple (R & K) could be tested through the same channel. Since the pyrotechnic event has to be captured within a short time period the data acquisition rate was set at 100 samples per second, with more than 1500 samples being recorded, depending on the test procedure.

It should be noted that initially a C-type thermocouple was also selected along with the R- and K-types because of their ability to withstand temperatures up to 2320 °C. The material used in the construction of these different types of thermocouples consists of two wires of:

- (a) platinum and the other platinum/rhodium alloy for the R-type,
- (b) tungsten and rhenium alloy for the C-type, and
- (c) chromel (a nickel chromium alloy) and alumel (a combination of nickel, aluminum, manganese and silicon) for the K-type.

However, from an initial investigation on the usage of a 0.217 mm (36-gauge) R-type thermocouple for

measuring the surface temperature of a common sparkler both the C- and R-type thermocouples were discarded in favour of the K-type. The reason for this decision may be considered from the following study where a 40 mm length of a standard 2.8 mm diameter sparkler has been mounted horizontally on an aluminum support. A second aluminum plate supports an R-type thermocouple such that the thermocouple bead is in contact with the surface of the sparkler, Figure 1.

However, it should be noted that once a sparkler is ignited, Figure 2, the visible sparking is created by the release of small iron particles that are distributed throughout its body and which may also be observed as physical protuberances

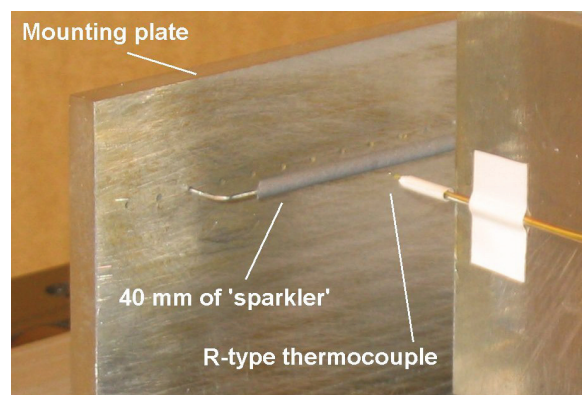


Figure 1 An R-type thermocouple touching the surface of a horizontally held sparkler.

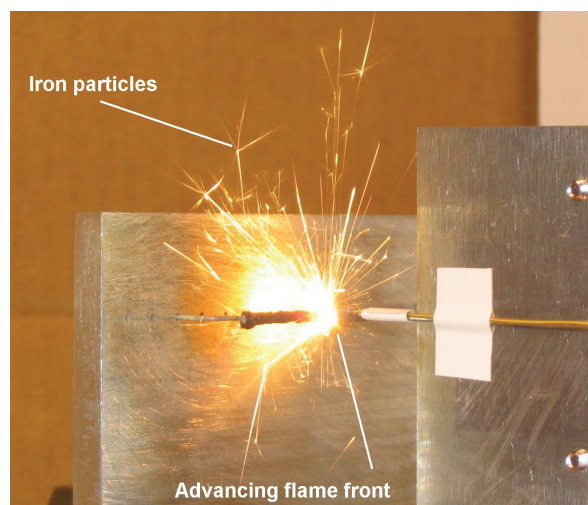


Figure 2 An advancing flame front passes over the R-type thermocouple bead.

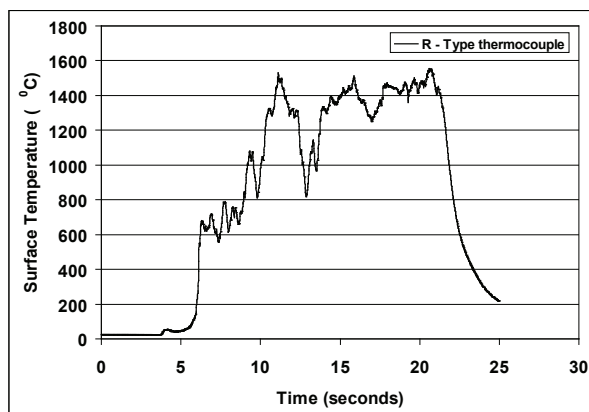


Figure 3 Surface temperature of a sparkler using an R-type thermocouple.

on its surface. In order that the thermocouple sensor could be located accurately against the sparkler surface these protrusions were removed before mounting the specimen in the supporting plate. As the flame front passes the thermocouple bead, the local surface temperature was recorded and a typical temperature–time plot is shown in Figure 3.

Here it is shown that as the flame front approaches the bead there is a rapid increase in temperature followed by series of temperature perturbations, reaching a maximum temperature of approximately 1575° C, before falling rapidly once the flame front has passed. These perturbations were considered related to the release of the small iron particles that, on their own, do not add to the heat generation but are likely to cause a local temperature fluctuation on their discharge. After considering the potential for large temperature errors to occur due to the contamination of the measuring bead at these high temperatures where the hot gases produced by the reaction cannot be controlled, a decision was made to discard their use in favour of the K-type thermocouple.

Similarly, a 0.217 mm (36-gauge) bare bead, unsheathed, C-type thermocouple was also examined, and not selected. Every attempt to sheath the bare wires resulted in damage to the thermocouple near the bead, due to the brittle nature and associated difficulty in handling of the wires. Furthermore, the tungsten wire required an inert atmosphere, since it also quickly oxidized at high temperatures.

The thermocouple eventually chosen was a 0.0787 mm diameter (40 gauge) K-type with an exposed bead weld junction. This thermocouple consists of two wires, which are insulated from each other except in the region of the bead, placed inside a sheath of 0.0762 mm thickness. The positive wire is made of chromel, which is a composition of 90% nickel and 10% chromium, and the negative wire is made of alumel, a composition of 95% nickel, 2% aluminum, 2% manganese and 1% silicon. The advantages of using the K-type thermocouples are:

- (1) They have the highest temperature range (–200 °C to 1250 °C) among the most commonly used types of thermocouples.
- (2) They could be fabricated within the laboratory. This was achieved by using pre-insulated wire and removing a 15 mm length of insulation from each. The exposed wires were then twisted and welded into a small bead in a thermocouple welder.

When the welded connection (bead) of a thermocouple is heated, a voltage across the two junctions is produced. A polynomial equation is then used to convert the thermocouple voltage (E) to a temperature ($T/^\circ\text{C}$) over a wide range of temperatures and is given by the equation based on the International Temperature Scale (ITS–90) standard:

$$T_{90}(E) = \sum_{i=0}^N d_i E^i$$

where the coefficients, d_i are as given by the National Bureau Standards in Table 2 below for K-type thermocouples.⁷

Time response evaluations of the K-type thermocouple

In order to be able to determine the time response of the chosen thermocouple a 50 mm × 50 mm square shock tube arrangement was used. The shock tube consisted of two sections, a closed high-pressure driver section and an open ambient pressure driven section, with a thin plastic diaphragm separating the two sections. By filling the driver section with high-pressure air until the plastic diaphragm bursts a shock, or blast, wave is produced that may travel at speeds greater than

Table 2 Polynomial coefficients for ITS-90 standard.

Type K polynomial coefficients	Value
i	d_i
0	0.226584602
1	24152.10900
2	67233.4248
3	2210340.682
4	-860963914.9
5	4.83506×10^{10}
6	-1.18452×10^{12}
7	1.38690×10^{13}
8	-6.33708×10^{13}

the speed of sound (approximately 330 m s^{-1} in air at standard temperature and pressure) through the driven section of the tube. At the exit of the driven section of the shock tube a small heat source (flame) is positioned with the test thermocouple situated close to its core such that it measures the local flame temperature. When the shock wave exits the driven section the flame is extinguished and the thermocouple experiences a step change in temperature from that of the flame (approximately $466 \text{ }^\circ\text{C}$) to that of the ambient temperature (approximately $21 \text{ }^\circ\text{C}$), Figure 4. The response time of the thermocouple is the time taken for the temperature to drop from the maximum temperature (T_{max}) to 63.2% of the final

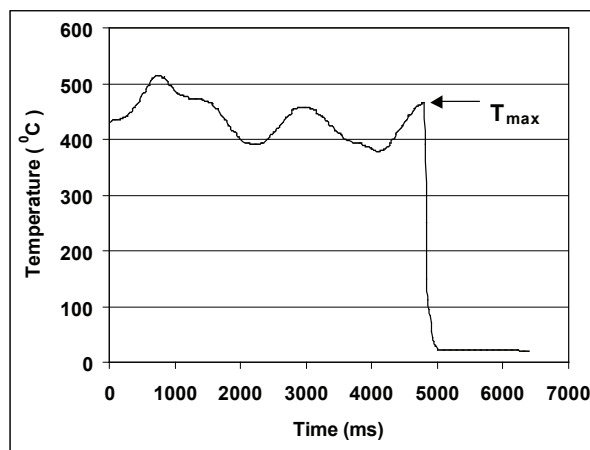


Figure 4 Thermal time response for a 40-gauge K-type thermocouple.

temperature. Several 0.0785 mm (40-gauge) K-type thermocouples were evaluated and their time constants determined to be approximately 10 ms.

Sparkler temperature profile analysis

Initially, tests were performed on commercially available sparklers that had a nominal diameter of 2.8 mm and prepared to a length of 40 mm, and located horizontally in the apparatus shown in Figure 1. Since the surface temperature was known to be as high as $1575 \text{ }^\circ\text{C}$, as measured previously with an R-type thermocouple, the locations of the K-type thermocouple were examined and it was concluded that they should be positioned no closer than 1.2 mm from the sparkler surface, and a typical temporal profile is shown in Figure 5. Here, it may be observed that as the flame approaches the thermocouple bead there is a steady rise in temperature until the flame is adjacent to the thermocouple where the maximum temperature is recorded. Once the flame passes the thermocouple the temperature falls to ambient conditions. However, due to the instability and pulsating nature of the flame an oscillation in the temperature profile can also be noted in this Figure.

Wasmann⁸ previously observed this fluctuating behavior of a pyrotechnic system and provided the explanation that two major factors were responsible for this action:

- (1) The competition between the various chemical reactions within the pyrotechnic composition.
- (2) Physical factors like heat loss, heat accumulation, and the intermittent vaporization

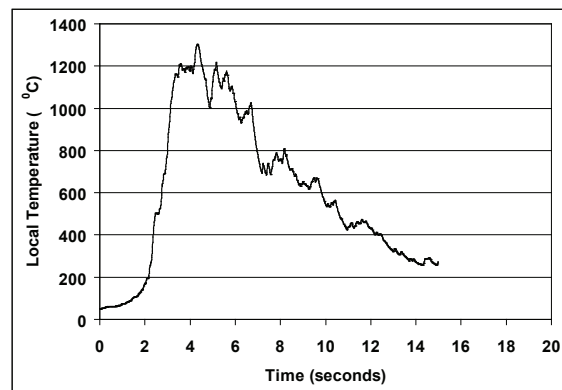


Figure 5 Temperature profile taken 1.2 mm away from a sparkler surface.

processes in the test composition.

In the first case, the pulsating flame behavior occurs as a result of competition in the chemical reaction and this may be explained as oscillations between light and dark cycles that occur when the composition consists of two or more different fuels. The quick reacting fuel reacts with the oxidizer releasing little energy in the form of light, hence representing a relatively dark cycle, whereas the light cycle is caused by large energy releases from the oxidation of the slow reacting fuel thereby producing large quantities of visible light. The rate of oxidation of the slow reacting component increases rapidly after the dark cycle due to the increase in the reaction surface area, and also due to the presence of oxidative gases from the dark cycle, trapped in the micro-porous structure of the surface. This dual cycle process seems to cause the pulsations in reactions with multiple fuel components, and with variable rates of reaction. In the case of sparklers, clear dark and light zones were not observed; however, the intensity of the emitted light could be seen to vary, and this pulsating behavior is observed as a change in emitted light intensity. In the chemical composition of the sparkler, the effect of the minor components has not been considered although these minor components may also affect the reaction rate by reacting with the oxidizer, thereby resulting in the dark phase of the pulsation cycle.

In the second case, the undulating nature of the temperature profile may be explained by the rapid heat loss from the surface following the release of an iron particle. This rapid thermal change would be sufficient to instantaneously lower the local temperature. Once the particle was released the surface temperature would again return to a quasi-steady state where the local temperature would attempt to return to its original value, albeit lower in value because of the passing of the flame front, before the release of another iron particle. The rate of release of the iron particles would provide the fluctuations in the temperature profile.

Although other physical properties like viscosity and volatility can also affect the burning process to create a pulsation effect as explained by Gol'binder and Goryachev,⁹ they were not considered in this study since there are no volatile components involved in the formation of the

standard sparkler.

In order to determine the temperature distribution around the surface of the sparkler, measurements were taken of the maximum attainable temperature at discrete locations in the $+x$, and $+z$ and $-z$ directions, where $+x$ refers to the horizontal distance radially away from the sparkler surface, and the $+z$ and $-z$ directions refer to the upper and lower vertical distances away from the sparkler surface respectively. Figure 6 shows diagrammatically the coordinate system adopted for these sets of measurements. These maximum temperatures were obtained in the three directions from more than 120 individual tests for a range of positions, from 1.15 mm to 2.5 mm in increments of 0.05 mm in the $+x$ direction and 0.10 mm in the $+z$ and $-z$ directions, Figures 7 and 8.

Although there is a large amount of scatter in the results, mainly due to the small differences in the composition of the charges, and the location of the thermocouple in relation to the sparkler surface, there is a distinct trend in the temperature distribution. From Figures 7 and 8, it may be observed that a drop in temperature occurs between 1.2 mm to 2.5 mm in both the x and z directions. Comparing the curve-fitted temperature profiles in the x and z directions, it may also be observed that the drop in the temperature in the z (vertical) directions is estimated to be some $170\text{ }^{\circ}\text{C mm}^{-1}$,

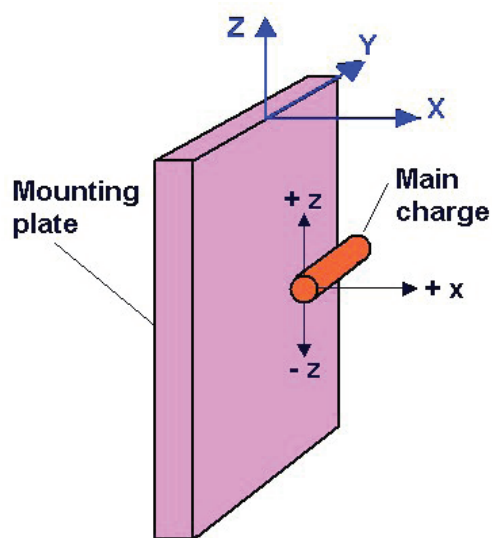


Figure 6 Coordinate system for the measurement of temperatures from the main charge (sparkler).

whereas in the x (horizontal) direction the fall in temperature is approximately 3 times greater. Furthermore, the temperature profiles shown in Figure 8 suggest that the thermal gradient in the $+z$ direction is less than that in the $-z$ direction, and may be explained by the following:

- (1) As the pyrotechnic materials melt in the reaction zone they tend to flow producing a downward shift in the sparkler's position due to its weight before complete combustion can occur. This effect reduces the distance between the thermocouple and the reacting pyrotechnic surface becoming more pronounced when the linear burning speed of the reaction zone, as it moves along the test sample, is low. In the current condition a burn speed of 2 mm s^{-1}

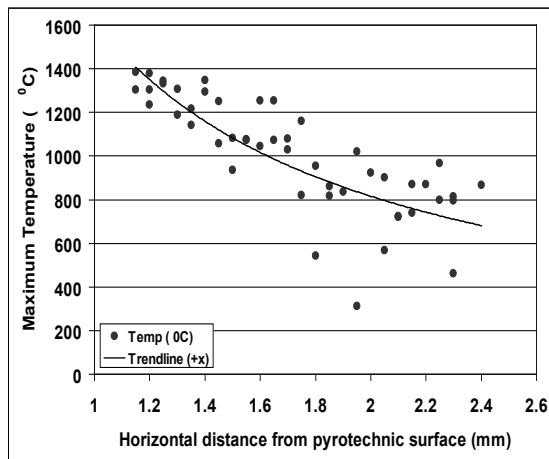


Figure 7 Temperature distribution in the horizontal $+x$ direction.

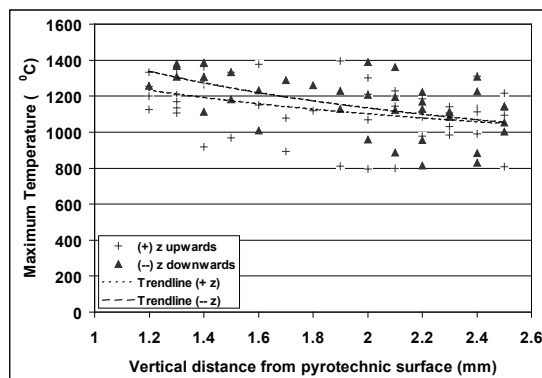


Figure 8 Maximum temperatures above and below the sparkler surface.

was recorded.

- (2) Effect of natural convection on the thermal field; similar to that observed around a heated horizontal cylinder by a Schlieren technique.

One of the difficulties of using standard sparklers was that of igniting the specimen accurately at a preset time. To overcome this obstacle, an electric match was formulated from two pyrotechnic components and attached to a main charge fabricated from sparkler material.

Test charge composition

The pyrotechnic material used in the main charge was obtained from commercial sparklers without the addition of the iron particles. The reason for removing these particles was to reduce the fluctuations in the temperature measurements previously observed and shown in Figures 3 and 5. This was achieved by crushing the sparklers into a fine powder and removing the iron particles with an electric magnet. The powder was then mixed with a chemical binder (dextrin) and moulded into a test charge, referred to as a commercial pyrotechnic material (CPM). The composition of this charge is given in Table 3: barium nitrate makes up 74% of the charge, and aluminum 24%, with 2% taken up with a chemical binder (dextrin).

Since it was intended to ignite the test charge in a more systematic manner, an electric match was fabricated with the main test charge. The pyrotechnic composition of the electric match is shown in Table 4: the oxidizer was potassium chlorate and the fuel was powdered lead thiocyanate. To hold the pyrotechnic compositions together a binder (dextrin) was again utilized.

Test charge fabrication

Once the main charge comprising the barium nitrate, aluminum and its binder was thoroughly mixed, it was pressed into a small cylindrical mould that had an internal diameter of 4 mm diameter, and was 15 mm long, for a length of 12 mm, with the remaining 3 mm allocated to the material for the 'electric match'. A steel support bar, 60 mm in length and 2 mm in diameter was then pushed through the mixture along the axis of the mold. An electric heating element consisting of a 50.8 mm long, 0.16 mm diameter (34-gauge)

Table 3 Chemical formulation of commercial pyrotechnic material.

Charge	Chemical	Formula	Quantity (by wt)	Mesh size
Main charge (CPM)	Barium nitrate	Ba(NO ₃) ₂	74%	<200
	Aluminum	Al	24%	<200
	Binder (dextrin)	(C ₆ H ₁₀ O ₅) _n	2%	<200

Table 4 Chemical composition of electric match.

Charge	Chemical	Formula	Quantity (by wt)	Mesh size
Electric match	Potassium chlorate	KClO ₃	55%	<200
	Lead thiocyanate	Pb(SCN) ₂	44%	<200
	Binder (dextrin)	(C ₆ H ₁₀ O ₅) _n	1%	<200

nichrome wire with a resistance of 2.73 ohm was wrapped around the support bar but isolated from it by a small piece of electrical insulating tape. The electric match mixture was then pushed into the remaining 3 mm part of the mold encompassing the electrical element such that the flat surface of the match composition is in contact with the composition of the main charge, around which the temperature distribution was to be measured. The complete test charge was then allowed to dry for 24 h and then removed from the mold. Ignition of the test charge was accomplished by igniting the electric match using the heating element connected to a 5 V DC power supply. Figure 9 is an image of the complete test charge showing the main charge, electric match, support bar and the electrical leads of the heating element.

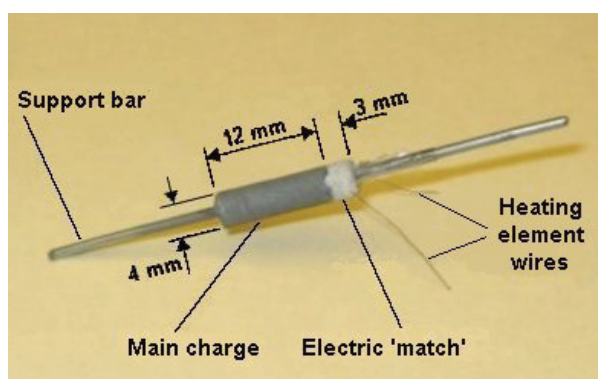


Figure 9 Image of fabricated CPM charge from sparkler material.

Testing facility

In order to improve the ability to locate a thermocouple bead away from the surface of the test charge with more accuracy a 3-dimensional traversing mechanism was constructed, Figure 10.

The base of the main traverse section supported the test charge holder, test charge, and three micrometer controlled slides to which three separate thermocouples could be mounted. The slides were configured to provide accurate independent

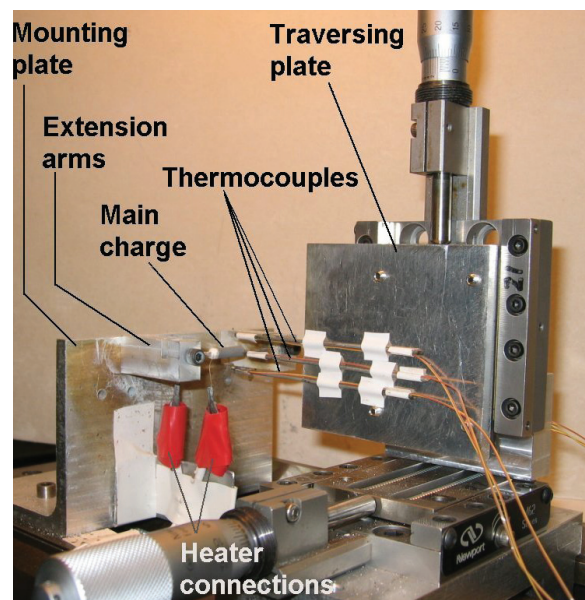


Figure 10 Facility for accurately positioning thermocouples close to the main charge.

movement in three orthogonal directions (x , y , z), with a spatial resolution in each direction of 1 micron. To allow the test charge to be rigidly fixed in space a separate aluminum mounting plate was utilized, and two extension arms added ensuring that the test charge was mounted off the plate by approximately 40 mm, Figure 10. In addition, a second flat rectangular traversing block was attached to the vertical segment of the traverse and acted as the base for multiple thermocouple attachment, as shown in Figure 10, thereby allowing multiple measurements to be made for any one test.

CPM temperature profile measurements

With a test charge mounted in the extension arms of the mounting plate an electrical connection to a 5 V DC power supply can be made to initiate the ignition process. Temperature measurements were taken using three K-type thermocouples arranged so that measurements could be obtained in the x -direction, and the $\pm z$ directions simultaneously at precise horizontal and vertical locations, Figure 6.

In this phase of the study the flame of the pyrotechnic was larger than the 2.8 mm diameter sparkler, which resulted in the burnout of the K-type thermocouples at approximately 2 mm from the surface of the test piece. Therefore in order to prevent continual thermocouple failure a larger standoff distance was utilized when compared

to the 2.8 mm diameter test charge. Figure 11 shows three temperature profiles around a 4 mm diameter test charge and it can again be observed that nearer the surface of the test charge, the magnitude of the temperature profile beneath the burning pyrotechnic (in the $-z$ direction) is larger than that above the charge (in the $+z$ direction), a trend similar to that found for the 2.8 mm diameter test species. However, the most striking feature of this data set is that the drop in temperature away from the burning test charge falls in a tight band with a nominal $200\text{ }^\circ\text{C}$ spread for all three directions, providing a temperature decay of approximately $240\text{ }^\circ\text{C mm}^{-1}$ over the distances measured. This is in contrast to the results found for the 2.8 mm diameter sparkler. However, there are small differences between the data sets and it may be inferred that the maximum decreases in temperature for all the three orientations occur in the x directions. The minimum drop may be observed in the $+z$ direction and the reason may be attributed to the flow of gases, due to natural convection, in this direction. The temperature drop in the $-z$ direction is between the temperature drop values in the other two directions, but below that for the $+z$ direction. The reasons for this relatively lower temperature drop in the $-z$ direction can be attributed to interference with natural convection from jet-like ejections, not related to the emission of iron particles.

The primary reason for the scatter in the data was due to the slight uncertainty in thermocouple position and the continuous pulsations in the flame when the premixed composition burned. Other factors that influence data scatter are related to the following initial assumptions:

- Each test piece has the same density/composition.
- Burning is uniform – following a ring-like pattern along the length of the test piece.
- Each test piece is unaffected by external conditions.

Although care was taken to maintain constant weight of each test charge, their weights varied within $\pm 2\%$ error. Similarly while compacting the composition into the mold shell, attempts were made to maintain the dimensions to within $\pm 2\%$, thereby keeping the test charge final density to

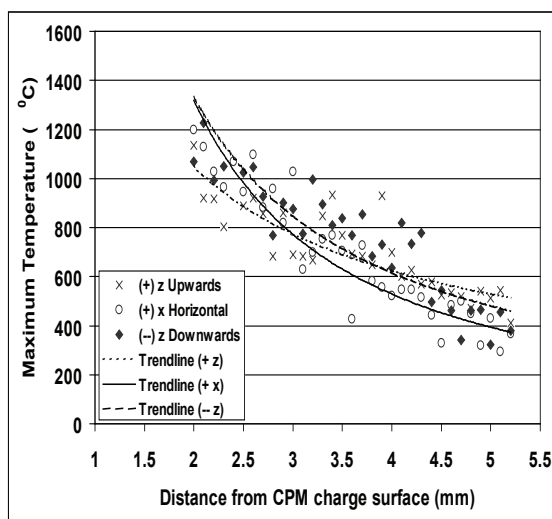


Figure 11 Temperature distributions around a 4 mm diameter CPM charge.

Table 5 Heat of formation for different chemical products.

Chemical formula	Chemical name	Heat of formation ΔH_f /kJ mol ⁻¹
Ba(NO ₃) ₂	Barium nitrate	-992
Al	Aluminum	0
BaO	Barium oxide	-548.1
Al ₂ O ₃	Aluminum oxide	-1675.7
N ₂	Nitrogen gas	0

within a couple of percent.

Furthermore, it was assumed that the ignition of the main charge occurred instantaneously from the initiator (electric match) with the resulting flame propagating uniformly through the entire cross-section of the main charge. In the absence of pulsations a ring-like burning pattern was assumed. However, if the flame does not cover the entire cross-section, an irregular burning pattern results and this can be exacerbated by the difference in the surface burning speeds. It was also assumed that changes in the ambient conditions, such as variations in temperature and forced convection, were small enough to be neglected.

It should also be noted that no temperature corrections due to conduction, convection and radiation have been applied to these measurements since it was considered that any error analysis would have been dependent on the thermal conductivity of the wires (k), the convective heat transfer coefficient (h) and the emissivity (ϵ) of the thermocouple sensor element. This dependence would have relied upon a steady state energy balance, a condition that was inappropriate for this dynamic situation. Furthermore, due to the gaseous nature of the pyrotechnic event, the convective heat transfer coefficient could not have been accurately determined; neither would the emissivity of the thermocouple bead be a single value due to the heating and cooling nature of the event discolouring the bead surface. However, as an approximation, a conduction error has been estimated from a simple energy balance between the net heat conducted along the wires and the heat convected to the wires. This analysis forms a simple second order differential equation that can be solved for the sensor temperature. For example, for a thermal conductivity of $24 \text{ W m}^{-1} \text{ deg}^{-1}$

for the wires, and $45.4 \text{ W m}^{-1} \text{ deg}^{-1}$ for the convective heat transfer coefficient, an error in the measurement of a bead temperature of $1200 \text{ }^\circ\text{C}$ would have been approximately $130 \text{ }^\circ\text{C}$, an error of some 10.8%. Likewise, an error in the temperature of the bead due to radiation has been estimated from a simple steady state energy balance between the convection heat transfer and the radiation transfer. This was achieved by using the above value for the convection heat transfer coefficient, and an emissivity value of 0.07 for a K-type (chromel/alumel) thermocouple, where it was found that the error in the temperature was approximately 1860 C , or 15.5%.

Summary

This work has shown that the near surface temperatures of a pyrotechnic charge may be measured accurately with miniature high-speed K-type thermocouples. Temperatures approaching $1600 \text{ }^\circ\text{C}$ were recorded at the surface of a 2.8 mm sparkler using an R-type thermocouple, while temperatures over $1300 \text{ }^\circ\text{C}$ were being measured 1.2 mm away from the sparkler surface using K-type thermocouples.

In the case of a standard sparkler the temperature distribution may be measured as close as 1.2 mm to the surface, whereas for the 4 mm diameter charge, made from the same material, the thermocouples could not be placed within 2.0 mm of the surface without a total failure.

When comparing Figures 7 and 8 for the 2.8 mm diameter sparkler to Figure 11 for the 4 mm charge, the temperature decay for the sparkler appears to have directional dependence and falls off more slowly than that for the 4 mm charge. It was also found that for the 2.8 mm sparkler the temperature decay in the vertical direction was approximately

30% lower compared to the temperature decay in the horizontal direction. This suggests that the heat liberation rate for the 2.8 mm charge was insufficient to overcome the energy transport by natural convection and thereby resulted in lower levels of thermal energy propagated in the horizontal direction.

The temperature around a 4 mm diameter test charge fabricated from commercially available pyrotechnic material has shown that, although there is a difference in the thermal energy being released in different directions, this difference is small compared with that obtained from the 2.8 mm sparkler, and that the temperature falls off in a tight band of approximately 200 °C.

References

- 1 A. A. Shidlovskiy, *Principles of pyrotechnics*, 3rd edition, 1964, English text prepared from translations by staff of *American Fireworks News*, Rex E. & S.P. Inc, 1997.
- 2 H. M. Strong, F. P. Bundy and D. A. Larson, "Temperature measurement on complex flames by sodium line reversal and sodium D line intensity contour studies", *3rd Symposium on Combustion and Flame and Explosion Phenomena*, 1949 , pp. 641–647.
- 3 M. W. Beck, "Temperature profile analysis of the Sb/KmnO₄ system", 14th International Pyrotechnics Seminar, Jersey, UK, 1989, pp. 433–442.
- 4 M. R. Birnbaum, "Determination of Pd/Al reaction propagation rates and temperatures", 6th International Pyrotechnics seminar, Colorado, USA, 1978, pp 39–61.
- 5 G. Pan, J. Hao, D. Jiang, and B. Su, "Measuring combustion temperature of high temperature (2000–2800 deg C) pyrotechnic compositions on W–Re thermocouple", 19th International Pyrotechnics seminar, Christchurch, NZ, 1994, pp. 52–56.
- 6 Y. L. Lao and P. Wang, "A study of pyrotechnic delay system and analysis of temperature profile", 13th International Pyrotechnics seminar, Colorado, USA, 1988, pp. 537–544.
- 7 T. J. Quinn, *Temperature*, Academic Press Inc., 1990.
- 8 F. W. Wasmann, "The phenomenon of pulsating burning in pyrotechnics", 5th International Pyrotechnics Seminar, Colorado, USA, 1976.
- 9 A. I. Gol'binder and V. V. Goryachev, "Pulsatory combustion of liquid explosives thickened with dissolved polymers", *Russian Journal of Physical Chemistry*, vol. 35, no. 8, 1961, pp. 889–891.